Improved thermoelectric properties of nanostructured composites out of $Bi_{1-x}Sb_x$ nanoparticles and carbon phases

Ekrem Güneş[1,7], Matthias T. Elm [2,3,4], Peter. J. Klar[2,3], Mathias S. Wickleder[6], Eckhard Müller[1,2,5]

[1]Institute of Inorganic and Analytical Chemistry, Justus-Liebig-University Giessen, Heinrich-Buff-Ring 17, 35392 Giessen, Germany

[2]Center for Materials Research, Justus-Liebig-University Giessen, Heinrich-Buff-Ring 16, 35392 Giessen, Germany

[3]Institute of Experimental Physics I, Justus-Liebig-University Giessen, Heinrich-Buff-Ring 16, 35392 Giessen, Germany

[4]Institute of Physical Chemistry, Justus-Liebig-University Giessen, Heinrich-Buff-Ring 17, 35392 Giessen, Germany

[5]Institute of Materials Research, German Aerospace Center (DLR), 51170 Köln, Germany

[6] Faculty of Mathematics and Natural Sciences, University of Cologne, Greinstrasse 6, 50939 Koeln, Germany

[7] E-mail: ekrem.guenes@anorg.chemie.uni-giessen.de

Abstract

Thermoelectric figures of merit of $ZT \approx 0.4$ at room temperature were achieved in nanostructured composite materials prepared by uniaxial pressing of $Bi_{1-x}Sb_x$ nanoparticles and 0.3 wt.% of a carbon phase. This constitutes a significant improvement of the low-temperature thermoelectric material $Bi_{1-x}Sb_x$ and strongly suggests the possibility of employing these materials in efficient thermoelectric devices working at room temperature. Interestingly, the beneficial effect of the carbon phase added to nanostructured $Bi_{1-x}Sb_x$ is the same for either carbon nanotubes or active carbon. This finding is attributed, on the one hand, to a combination of electronic band gap engineering due to nanostructuring and energy filtering due to graphene-like interlayers between $Bi_{1-x}Sb_x$ grains and, on the other hand, to modified phonon scattering at the grain boundaries and additional phonon scattering by agglomeration sites of carbon material on the µm scale.

Introduction

The growing demand of energy and the society's awareness of environmental issues such as global warming constitute driving forces for tapping renewable energy sources such as sun light or wind instead of fossil fuels [1, 2], but also for improving the efficiency of existing energy conversion processes [3, 4, 5]. Thermoelectric generators possess the potential of

converting an additional fraction of the large amounts of unused waste heat of combustion processes in automobiles, industrial plants, and other facilities into electricity and thus to diminish these losses. However, the still rather low efficiency of thermoelectric generators restricts a wide and economically viable application. The efficiency of the thermoelectric generator depends largely on the dimensionless thermoelectric figures of merit of the materials employed in its p-type and n-type legs. The thermoelectric figure of merit *ZT* of a material is defined as $ZT = S^2\sigma T/\kappa$ where σ, S, and κ denote the electrical conductivity, the Seebeck coefficient, and thermal conductivity, respectively. Best conventional thermo-electric bulk materials barely reach a *ZT* of 1; values of at least 2 need to be targeted for thermoelectric technologies to become of interest on a mass market scale. [6]

Different strategies are currently pursued in the quest for materials with a higher *ZT*. [6, 7, 8, 9] A promising strategy is to employ hybrid structures where the thermoelectric properties are tuned by combining two constituents. If the hybrid formation takes place on the nanoscale or mesoscale, it will often be found that the resulting thermoelectric properties deviate significantly from those predicted by effective medium theory. [10, 11] This finding indicates that the interfaces between the constituents play a significant role in the transport processes of charge carriers and phonons determining the transport coefficients σ, S, and κ. [12] For example, hybrid materials may be obtained by thermally induced segregation of nanoinclusions in a bulk material or by mixing nanostructures of different origin and compacting the mixture by hot or cold pressing. The latter approach yields more degrees of freedom as the various nanostructures combined can be chosen more or less freely in terms of composition and morphology, e.g. nanoparticles, nanowires or nanotubes etc.

Carbon nanotubes (CNT) are often chosen as one constituent of such hybrid materials. The choice is driven by their unusual mechanical, thermal and electrical properties. [10, 18, 19, 20, 21, 22, 23] We have recently demonstrated that nanostructured composites of CNT and $Bi_{1-x}Sb_x$ nanoparticles exhibit considerably improved thermoelectric properties. [24] Here, we show that nanostructured composites of active carbon (AC) and $Bi_{1-x}Sb_x$ nanoparticles (i.e. where AC replaces CNT in the composites) exhibit similar thermoelectric properties than the original $Bi_{1-x}Sb_x$/CNT composites. These findings suggest that the improvement of the thermoelectric properties of $Bi_{1-x}Sb_x$/CNT nanostructured composites compared to nanostructured $Bi_{1-x}Sb_x$ reference samples is not related to the tubular structure of CNT or a resulting CNT network interpenetrating the nanostructured $Bi_{1-x}Sb_x$ but rather to carbon-related modifications of the interfaces between the $Bi_{1-x}Sb_x$ nanoparticles.

Experimental Part

Synthesis

$Bi_{1-x}Sb_x$ nanoparticles with x = 0.1, 0.12, 0.13, 0.15, and 0.2 were synthesized by ball-milling of powders of the elemental constituents (bismuth: 99,5 % Alfa Aesar; antimony: 99,5% Roth). For this, the weighed amounts of the powders were transferred into a stainless steel milling container and sealed under argon atmosphere (glove box). It followed a twenty-hour

ball-milling procedure using a powder-volume-ration of 7,5 : 1 and 450 revolutions perminute (rpm). After ball-milling the powders were removed under inert gas and subsequently transferred into a Schlenk tube, where they were tempered for 17 hours at 250 °C under a gentle argon stream. [17, 24, 25] A detailed characterization of the $Bi_{1-x}Sb_x$ nanoparticles can be found in Ref. 24. In brief, the $Bi_{1-x}Sb_x$ nanoparticles were crystalline, alloy formation took place, and the nanoparticles were between 50 nm and 100 nm in diameter.

After synthesis, the $Bi_{1-x}Sb_x$ matrix material was mixed with 0.3 wt.% of either CNT (Baytubes C70P) or AC (Merck Millipore). Weighing of the educts was realized under argon atmosphere in a glove box. A content of 0.3 wt.% of the carbon phase was chosen because $Bi_{1-x}Sb_x$/CNT composites with 0.3 wt.% of CNT were found to be less brittle than composite samples with higher CNT contents and already showed a *ZT* enhancement by a factor of about 2.5 compared to the reference samples without CNT. [24] The mixtures were pressed for two hours at a pressure of 780 MPa and at a temperature of 50 °C to form pellets of cylindrical shape. After the pressing process the samples were pestled and pressed again to achieve a high degree of homogeneity. The second pressing step lasted for three hours using the same conditions (50 °C, 780 MPa) than during the first pressing step. For all five compositions *x* and both carbon materials, we prepared two pellets of different shape to enable us to determine all three transport coefficients along the *y*-direction, i.e. perpendicular to uniaxial pressing direction *z*. In Ref. 24, we reported an anisotropy of the transport properties of the nanostructured $Bi_{1-x}Sb_x$/CNT composites introduced by the uniaxial pressing procedure. There, it turned out that the *ZT* values of the composite samples obtained for transport along the *y*-direction were superior to those found for transport along *z*. The pellets were tempered for 17 hours at 250 °C to ensure the recovery and relaxation of the material from the mechanical strain caused by the pressing process. In addition, we prepared nanostructured $Bi_{1-x}Sb_x$ reference samples for all five compositions *x*.

Characterization of the microstructure

The microstructure of the $Bi_{1-x}Sb_x$/CNT and $Bi_{1-x}Sb_x$/AC composites as well as of the $Bi_{1-x}Sb_x$ reference samples was further investigated using scanning electron microscopy (SEM, JEOL JSM 7001F) with an acceleration voltage of 15 keV. Figure 1 shows typical SEM images of the three kinds of samples. Figure 1 (a) shows that the pellet surface of the reference samples is smooth and dense down to the 1 µm scale. High compactness with only a low degree of microstructural defects from the millimeter scale down to the micrometer scale is found for all reference samples. Images recorded with a 100 times lower magnification of pellets of $Bi_{1-x}Sb_x$/CNT and $Bi_{1-x}Sb_x$/AC composites are shown in Figs. (b) and (c), respectively, and demonstrate a similar level of compactness from the millimeter down to 100 µm scale. However, both images also reveal isolated structural defects on the 1 µm scale which in both cases correspond to agglomerations of the carbon materials. Figs. (d) and (e) are close views of higher magnification of such agglomerations and show the interconnected CNT bundles and layered AC material, respectively. Thus the microstructure of the inclusion materials is to

a large extent preserved at these agglomeration sites. As the agglomeration sites are separated by µm distances and thus do not form a close network pervading the entire composite sample their impact on the electronic transport properties should be rather weak. This is in accordance with the temperature-dependent magneto-transport results reported for the $Bi_{1-x}Sb_x$/CNT composites in Ref. 24 which are very similar to those of $Bi_{1-x}Sb_x$ reference samples and can be consistently explained by temperature, composition and confinement-induced changes of the $Bi_{1-x}Sb_x$ band structure. [14, 15, 16] However, the agglomeration sites may act as scattering centers for phonons with small wave vectors.

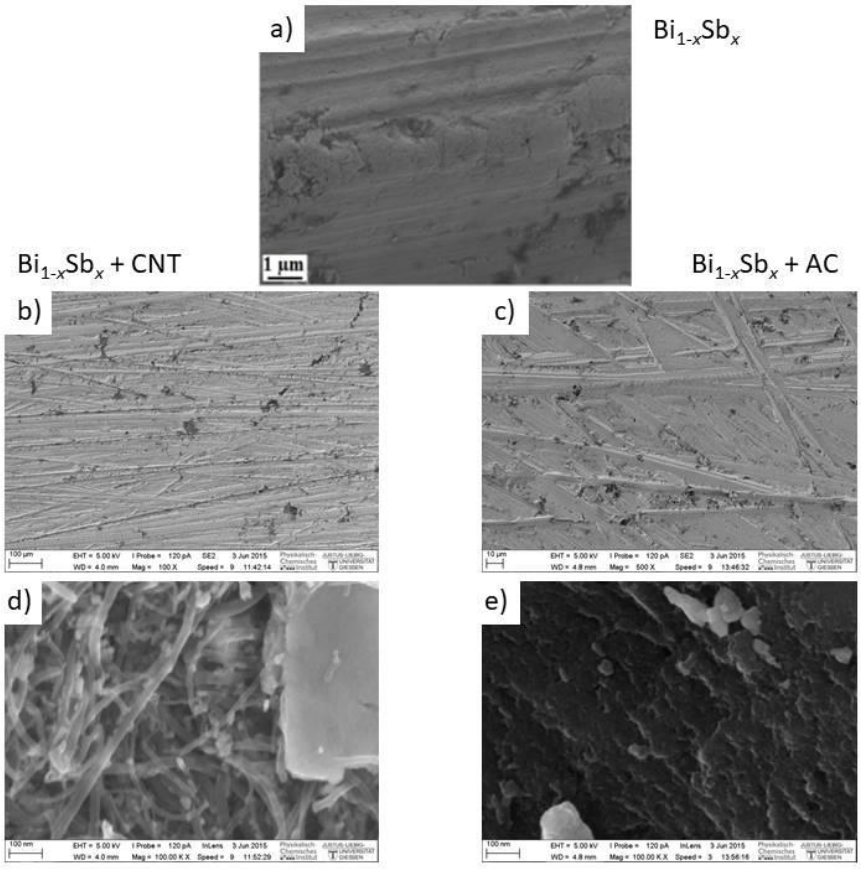

Fig. 1: (a) SEM-image of the surface of a pellet prepared from $Bi_{1-x}Sb_x$ nanoparticles alone. (b) and (d) SEM-images of the surface of a pellet of a $Bi_{1-x}Sb_x$/CNT composite at two different magnifications. (c) and (e) SEM-images of the surface of a pellet of a $Bi_{1-x}Sb_x$/AC composite at two different magnifications.

Characterization of the thermoelectric properties

Magneto-transport measurements were performed in the temperature range between 30 and 300 K using a superconducting magnet system (Oxford) generating magnetic fields up to 10 T. The electrical conductivity of the composites was measured in van der Pauw geometry with indium contacts soldered onto the sample surface and with the magnetic field applied perpendicular to the sample surface. The thermal conductivity was determined from the thermal diffusivity measured using a Linseis XFA (Linseis, Selb Germany). The Seebeck coefficient was determined between 120 und 310 K using a custom-made setup. Between 300 and 473 K the Seebeck coefficient and the electrical conductivity were measured

simultaneously in four-point geometry using a LSR-3 device (Linseis, Selb Germany). All transport coefficients of the composites were measured along the *y*-direction.

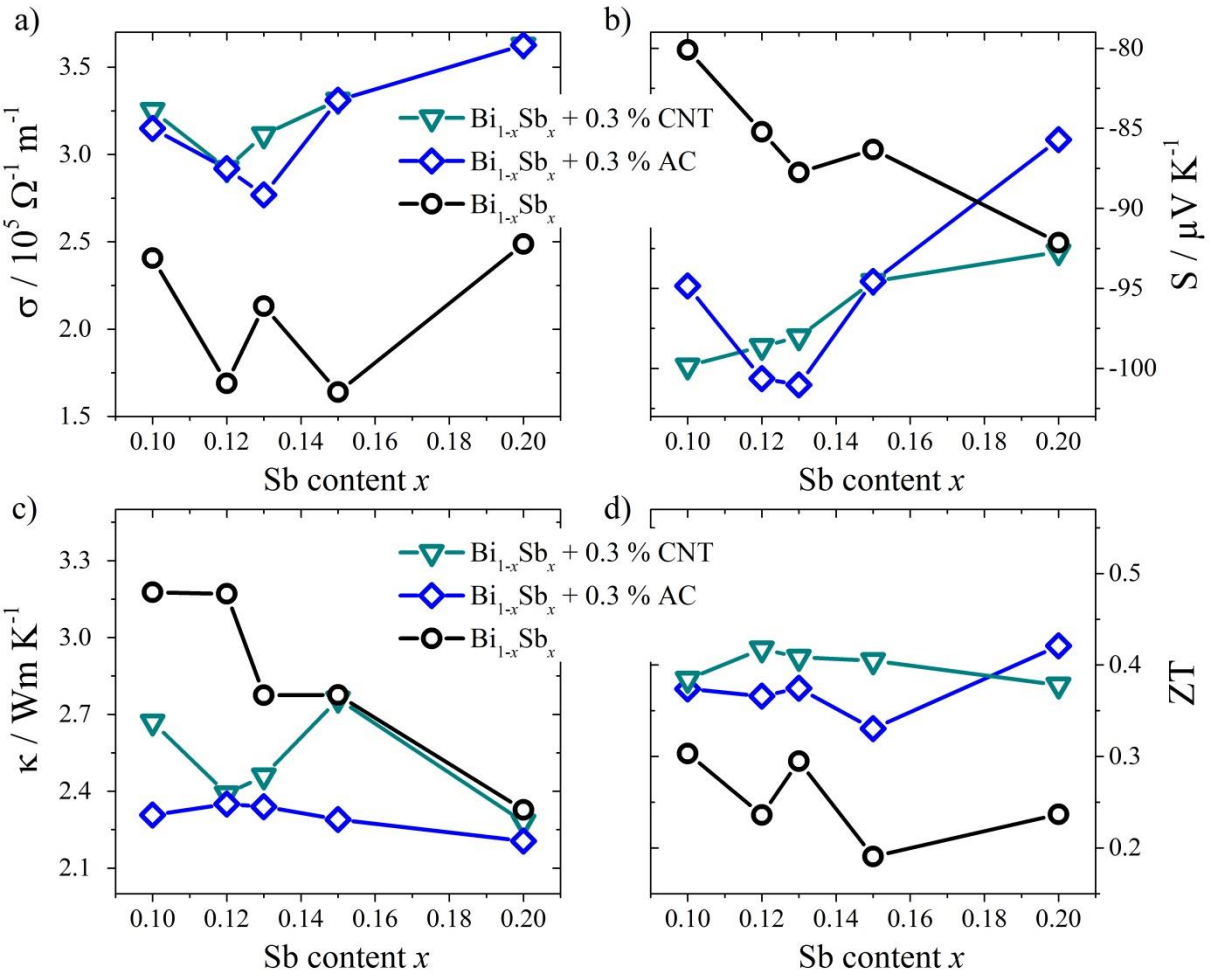

Fig. 2: Room-temperature thermoelectric properties of $Bi_{1-x}Sb_x$/CNT (triangles) and $Bi_{1-x}Sb_x$/AC composites (diamonds) as well as of the nanostructured $Bi_{1-x}Sb_x$ reference samples (circles); a) electrical conductivity, b) Seebeck coefficient, c) thermal conductivity, and d) Figure of Merit.

Figure 2 summarizes the room-temperature thermoelectric properties of the three types of samples, ($Bi_{1-x}Sb_x$/CNT and $Bi_{1-x}Sb_x$/AC composites as well as of the nanostructured $Bi_{1-x}Sb_x$ reference samples) as a function of Sb content *x*. As a trend, incorporation of the carbon material increases the electrical conductivity σ, increases the absolute value of the Seebeck coefficient *S*, but decreases the thermal conductivity κ, leading to a rise of the *ZT* value at room temperature from about 0.15 for conventional crystalline material to about 0.4 as shown in Fig. 3d). [13, 24] This is about half the room-temperature *ZT* value of that of Bi_2Te_3 based materials which are currently employed in thermoelectric devices used at temperatures close to room temperature. [26, 27]

It should be noted that the *ZT* values obtained are within the experimental uncertainty independent of the type of carbon material used. In particular, we can rule out that the *ZT* enhancement observed in the two series of composite samples is related to the special mechanical, thermal and electrical properties of CNTs as AC possesses an entirely different morphology, but yields similar results. Furthermore, all three series of samples exhibit negative Seebeck coefficients at room temperature. Thus, the electronic transport of the

nanostructured composites as well as of the nanostructured reference material is dominated by high-mobility electrons excited across the small band gap at this temperature. This finding is further corroborated by the results shown in Fig. 3.

Fig. 3 summarizes the results of the low-temperature transport measurements. As an example, Fig. 3 (a) displays temperature-dependent measurements of the electrical conductivity of $Bi_{1-x}Sb_x$/AC composite samples of different *x*. The temperature dependence observed is typical for $Bi_{1-x}Sb_x$ alloys. [16, 24, 25] At low temperatures a nearly constant conductivity is found. It is likely due to the formation of an impurity band probably caused by impurities in the reactants used in the synthesis process. With increasing temperature the conductivity increases revealing a semiconducting behavior. At temperatures above 300 K the composites exhibit a metal-like behavior due to their small band gap, where the decrease in conductivity can be attributed to increasing phonon scattering. In the semiconducting temperature range (100 K to about 200 K) the thermal band gaps of the composites were estimated from the slope of a linear fit in an Arrhenius representation of the conductivity (inset in Fig. 3 a)). The thermal band gaps determined for the two series of composite samples as well as for the nanostructured reference samples are shown in Fig. 3 b) as a function of Sb content *x*. For all three series, a maximum of the thermal band gap occurs for an Sb content of about 12 to 13% as known for bulk $Bi_{1-x}Sb_x$ alloys. Thus, the inclusion of carbon material has no significant effect on the composition dependence of the band structure of the nanostructured matrix material, but it changes the magnitude of the band gaps, i.e. leads to a stronger confinement of the electronic states in the $Bi_{1-x}Sb_x$ nanoparticles forming the samples.

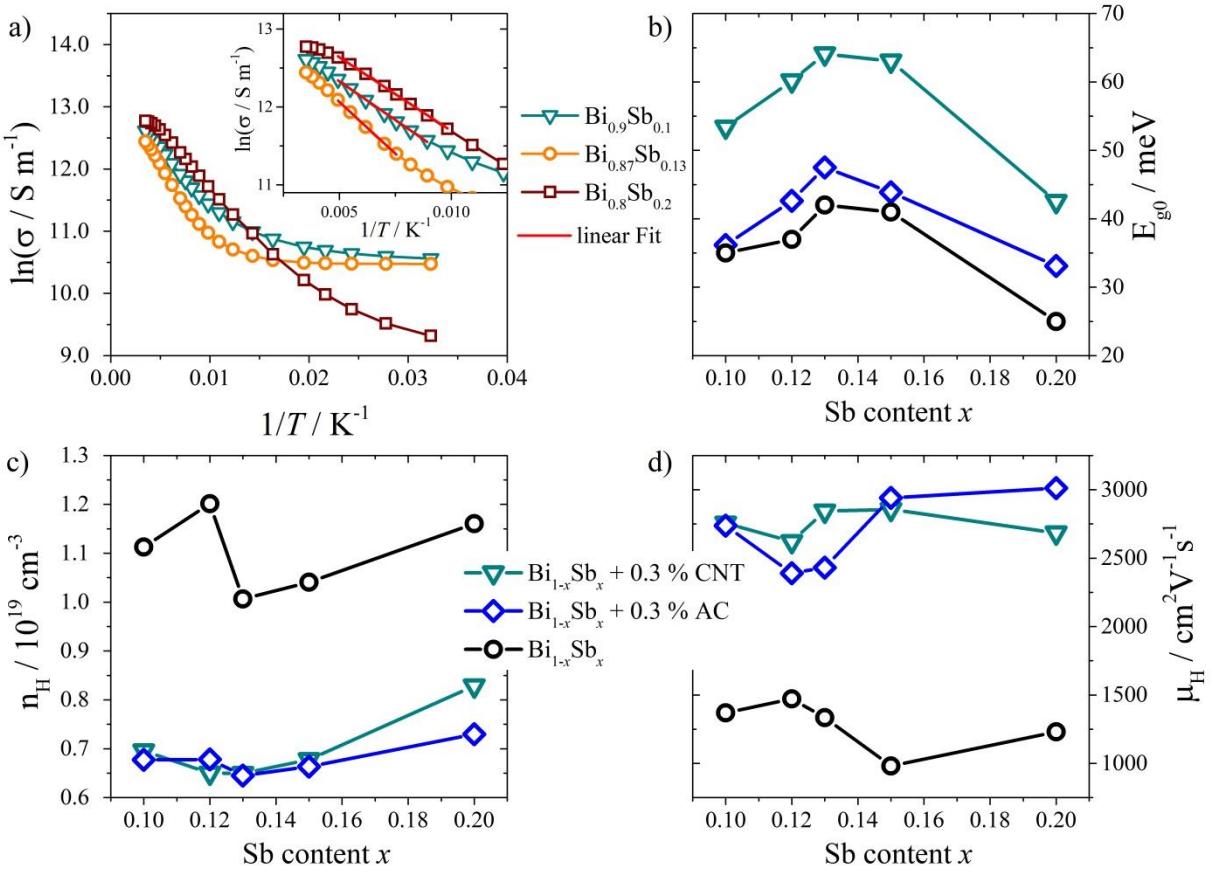

Fig. 3: (a) Temperature dependence of the electrical conductivity of the sample series $Bi_{1-x}Sb_x$ with 0.3 wt.% AC for different *x*. The inset shows the linear fit in the temperature from 100 to 200 K. b) Thermal band gaps, c) effective carrier concentration, and d) Hall mobility of $Bi_{1-x}Sb_x$/AC, $Bi_{1-x}Sb_x$/CNT, and nanostructured $Bi_{1-x}Sb_x$ reference samples as a function of *x*.

The effective carrier concentration n_H (Fig. 3c)) as well as the Hall mobility μ_H (Fig. 3 d)) were extracted from the magneto-transport data at high magnetic fields assuming a simple Drude model, i.e. the ambipolar transport properties of $Bi_{1-x}Sb_x$ alloys [15, 16, 28] were neglected. Thus, the values obtained only represent an effective carrier concentration and somewhat correspond to the difference between majority and minority carriers in the different bands. In all samples, electrons are the majority carriers at room temperature due to the small band gap and higher mobilities compared to holes. The behavior of the effective carrier concentration is almost the same for all three series of samples and can mainly be attributed to the changes of the band structure with Sb content. With increasing thermal band gap, i.e. increasing Sb content, the carrier concentration decreases reaching a minimum for an Sb content of about 13%, where the largest band gap is observed in each series. The reduction of the thermal band gap observed at higher Sb content again correlates with a rise of the effective carrier concentration. Furthermore, when comparing the mobility values of the two series of composite samples to those of the nanostructured reference material a significant enhancement of the mobility values in the composites is found.

The beneficial effect of the carbon inclusion on the mobilities of the majority charge carriers may be attributed to graphene-like abrasion products formed during the pestling. [24] These products can form a carbon coating on the single $Bi_{1-x}Sb_x$ surface which may act as energy

barriers between the grains. Then, low energy electrons cannot pass the energy barriers resulting in an energy filtering effect and thus in a significant increase of the mobility of the charge carriers due to reduced electron-electron scattering. [30, 31, 32, 33]

In a simple model the Seebeck coefficient depends reciprocal on the carrier concentration. [34] This correlation between Seebeck coefficient and carrier concentration (i.e. band gap) is reflected in the composition dependence of the Seebeck coefficient at 300 K for all three series of samples investigated. Maxima of the thermal band gap as a function of composition *x* are found close to an Sb content of 13 %, where the samples possess the lowest effective carrier concentrations and correspondingly exhibit the highest absolute values of the Seebeck coefficient. Energy filtering not only increases the mobility of the charge carriers, but also reduces the effective carrier concentration. [30] Thus, the larger absolute values of the Seebeck coefficients in conjunction with lower effective carrier concentrations in the composites compared to the nanostructured reference samples support the assumption of a carbon-like layer between the $Bi_{1-x}Sb_x$ nanoparticles of the composites.

The inclusion of carbon materials in the composites also results in a remarkable reduction of κ for all compositions investigated. Especially for low Sb content a reduction of the thermal conductivity of about 25% is observed. The modification of the boundaries between the $Bi_{1-x}Sb_x$ nanoparticles by carbon is likely to contribute to this effect. However, the variation of the content of the carbon phase in the composite also revealed a correlation between the density of the agglomeration sites and the reduction of the thermal conductivity. Thus, we believe that the existence of the agglomeration sites, which act as additional scattering centers for phonons, also contributes the reduction of κ observed in the composites compared to the nanostructured references.

Summary

Nanostructured composite materials prepared by compacting mixtures of $Bi_{1-x}Sb_x$ nanoparticles with carbon phases such as CNT or AC possess thermoelectric properties superior to those of the nanostructured $Bi_{1-x}Sb_x$ reference samples. The thermoelectric properties of nanostructured $Bi_{1-x}Sb_x$/CNT and $Bi_{1-x}Sb_x$/AC composites of the same *x* and mass fraction of the carbon phase are very similar despite the morphological differences between CNT and AC. The experimental data can be consistently explained by the formation of carbon-like layers between the $Bi_{1-x}Sb_x$ nanoparticles of the composites accompanied by the formation of agglomeration sites of the carbon material on the µm scale. The modification of the grain boundaries by carbon leads to energy filtering effects which are advantageous for the electronic transport coefficients and possibly reduce the thermal conductivity. The agglomeration sites add another contribution to the reduction of the thermal conductivity by acting as additional scattering centers for phonons. As the morphology or dimensionality of the carbon inclusion material (CNT vs. AC) is not important, active carbon represents a cheap alternative to carbon nanotubes for tuning the micro- and nanostructural properties of these thermoelectric composite materials. Furthermore, the

significant increase of the figure of merit may establish nanostructured $Bi_{1-x}Sb_x$ composites with AC inclusions as thermoelectric materials also for room temperature applications. The *ZT* values of about 0.4 achieved for the composites at room temperature are almost three times larger than those of the nanostructured reference samples. More importantly, the *ZT* values achieved are about half of the room-temperature *ZT* value of Bi_2Te_3 bulk material which is currently employed in thermoelectric devices for applications close to room temperature.

References

[1] Khan J, Arsalan MH., Solar power technologies for sustainable electricity generation – A review. *Renewable and Sustainable Energy Reviews*. 2016; **55**: 414-425

[2] Kumar Y, Ringenberg J, Depuru SS, Devabhaktuni VK, Lee JW, Nikolaidis E, Andersen B, Afjeh A, Wind energy: Trends and enabling technologies. *Renewable & Sustainable Energy Reviews*. 2016. **53**: 209-224

[3] Bell LE. Cooling, Heating, Generating Power, and Recovering Waste Heat with Thermoelectric Systems. *Science*. 2008;**321**:1457-61.

[4] Schlecht S, Böttner H. Energiewandler mit großem Zukunftspotenzial. *Nachrichten aus der Chemie*. 2008;**56**:136-9.

[5] Minnich AJ, Dresselhaus MS, Ren ZF, Chen G. Bulk nanostructured thermoelectric materials: current research and future prospects. *Energy & Environmental Science*. 2009;**2**:466-79.

[6] Vineis CJ, Shakouri A, Majumdar A, Kanatzidis MG. Nanostructured Thermoelectrics: Big Efficiency Gains from Small Features. *Adv. Mater.* 2010; **22**:3970.

[7] Sootsman JR, Chung DY, Kanatzidis MG. Alte und neue Konzepte für thermoelektrische Materialien. *Angew. Chem*. 2009; **121**:8768

[8] Snyder GF, Toberer ES. *Complex thermoelectric materials*. Nature Mater. 2008;**7**:105

[9] Kanatzidis MG. Nanostructured Thermoelectrics: The New Paradigm? *Chem. Mater.* 2010;**22**:648-59.

[10] R. Nunna, P. Qiu, M. Yin, H. Chen, R. Hanus, Q. Song, T. Zhang, M.-Y. Chou, M.T. Agne, J. He, G.J. Snyder, X. Shi, L. Chen. Ultrahigh thermoelectric performance in Cu_2Se-based hybrid materials with highly dispersed molecular CNTs. *Energy & Environ. Sci.* 2017; **10**:1928-1935.

[11] M. T. Elm, T. Henning, P. J. Klar, and B. Szyszka. Effects of artificially structured micrometer holes on the transport behavior of Al-doped ZnO layers. *Appl. Phys. Lett*. 2008; **93**:232101.

[12] F. Gather, C. Heiliger, P.J. Klar. NeMo: A network model program for analyzing the thermo-electric properties of meso and nanostructured composite materials. *Prog. Solid State Chem*. 2011; **39**:97-107.

[13] Smith GE, Wolfe R. Thermoelectric Properties of Bismuth-Antimony Alloys. *Journal of Applied Physics*. 1962;**33**:841-6.

[14] Chao PW, Chu HT, Kao YH. Nonlinear band-parameter variations in dilute bismuth-antimony alloys. *Physical Review B*. 1974;**9**:4030-4.

[15] Oelgart G, Schneider G, Kraak W, Herrmann R. The Semiconductor-Semimetal Transition in $Bi_{1-x}Sb_x$ Alloys. *physica status solidi (b)*. 1976;**74**:K75-K8.

[16] Will CH, Elm MT, Klar PJ, Landschreiber B, Güneş E, Schlecht S. Effect of nanostructuring on the band structure and the galvanomagnetic properties in $Bi_{1-x}Sb_x$ alloys. *J. Appl. Phys*. 2013;**114**:193707.

[17] Landschreiber B, Güneş E, Rohner C, Homm G, Will C, Sesselmann A, Klar PJ, Müller E, Schlecht S. Comparison of the structural and thermoelectric properties of ball-milled and co-reduced $Bi_{1-x}Sb_x$ nanoalloys. *AIP Conference Proceedings*. 2012;**1449**:303-6.

[18] Zhan G-D, Kuntz JD, Mukherjee AK, Zhu P, Koumoto K. Thermoelectric properties of carbon nanotube/ceramic nanocomposites. *Scripta Materialia*. 2006;**54**:77-82.
[19] Meng C, Liu C, Fan S. A Promising Approach to Enhanced Thermoelectric Properties Using Carbon Nanotube Networks. *Advanced Materials*. 2010;**22**:535-9.
[20] Yao Q, Chen L, Zhang W, Liufu S, Chen X. Enhanced Thermoelectric Performance of Single-Walled Carbon Nanotubes/Polyaniline Hybrid Nanocomposites. *ACS Nano*. 2010;**4**:2445-51.
[21] Yu C, Kim YS, Kim D, Grunlan JC. Thermoelectric Behavior of Segregated-Network Polymer Nanocomposites. *Nano Letters*. 2008;**8**:4428-32.
[22] Zhang K, Zhang Y, Wang S. Enhancing thermoelectric properties of organic composites through hierarchical nanostructures. *Scientific Reports*. 2013;**3**:3448.
[23] Ren F, Wang H, Menchhofer PA, O. Kiggans J. Thermoelectric and mechanical properties of multi-walled carbon nanotube doped $Bi_{0.4}Sb_{1.6}Te_3$ thermoelectric material. *Appl. Phys. Lett*. 2013; **103**: 221907.
[24] Güneş E, Gundlach F, Elm MT, Klar PJ, Schlecht S, Wickleder MS, Müller E. Nanostructured composites of $Bi_{1-x}Sb_x$ nanoparticles and carbon nanotubes and the characterization of their thermoelectric properties. ACS Appl. Mater. Interfaces. 2017; **9**: 44756.
[25] Güneş E, Landschreiber B, Hartung D, Elm MT, Rohner C, Klar PJ, Schlecht S. Effect of Bismuth Nanotubes on the Thermoelectric Properties of BiSb Alloy Nanocomposites. *J. Electron. Mater*. 2014;**43**:2127-33.
[26] Scherrer S, Scherrer H. Bismuth Telluride, Antimony Telluride, and Their Solid Solutions in Rowe DM, CRC Handbook of Thermoelectrics: CRC Press; 1995.
[27] Wu Y, Zhai R, Zhu T, Zhao X. Enhancing room temperature thermoelectric performance of n-type polycrystalline bismuth-telluride-based alloys via Ag doping and hot deformation *Materials Today Physics*. 2017; **2**:62.
[28] Lenoir B, Cassart M, Michenaud JP, Scherrer H, Scherrer S. Transport properties of Bi-RICH Bi-Sb alloys. *J. Phys. Chem. Solids*. 1996;**57**:89-99.
[29] Makongo JPA, Misra DK, Zhou X, Pant A, Shabetai MR, Su X, Uher C, Stokes KL, Poudeu PFP. Simultaneous Large Enhancements in Thermopower and Electrical Conductivity of Bulk Nanostructured Half-Heusler Alloys. *J. Am. Chem. Soc*. 2011;**133**:18843-52.
[30] Makongo JPA, Misra DK, Zhou X, Pant A, Shabetai MR, Su X, Uher C, Stokes KL, Poudeu PFP. Simultaneous Large Enhancements in Thermopower and Electrical Conductivity of Bulk Nanostructured Half-Heusler Alloys. *Journal of the American Chemical Society*. 2011;**133**:18843-52.
[31] Nishio Y, Hirano T. Improvement of the Efficiency of Thermoelectric Energy Conversion by Utilizing Potential Barriers. *Jpn J. Appl. Phys*. 1997;**36**:170.
[32] Paul B, V AK, Banerji P. Embedded Ag-rich nanodots in PbTe: Enhancement of thermoelectric properties through energy filtering of the carriers. *Journal of Applied Physics*. 2010;**108**:064322.
[33] Soni A, Shen Y, Yin M, Zhao Y, Yu L, Hu X, Dong Z, Khor KA, Dresselhaus MS, Xiong Q. Interface Driven Energy Filtering of Thermoelectric Power in Spark Plasma Sintered $Bi_2Te_{2.7}Se_{0.3}$ Nanoplatelet Composites. *Nano Letters*. 2012;**12**:4305-10.
[34] Cutler M, Leavy JF, Fitzpatrick RL.Electronic Transport in Semimetallic Cerium Sulfide. *Phys. Rev.* 1964;**133**:A1143.